

# Silicon Nitride Nanostructures Prepared from n-type and p-type Silicon Targets

Diyar A. Taher <sup>1</sup>, Mohammed A. Hameed <sup>2</sup>

<sup>1</sup> Al-Kindi State Hospital, Ministry of Health, Baghdad, IRAQ

<sup>2</sup> Department of Physics, College of Science, University of Baghdad, Baghdad, IRAQ

## Abstract

Silicon nitride nanostructures were prepared by reactive sputtering technique using silicon targets with different types of electrical conductivity (n-type and p-type) and Ar:N<sub>2</sub> gas mixing ratio of 70:30. The optical microscopy and spectroscopic characteristics of these films were determined in order to introduce the effect of target conductivity type on these characteristics. The results showed that using p-type silicon target would produce Si<sub>3</sub>N<sub>4</sub> films with lower tendency to adsorb water vapor and other constituents of the atmospheric air, higher absorbance in the visible range 400-700nm, and lower variation in the energy band gap with film thickness than the Si<sub>3</sub>N<sub>4</sub> films prepared from n-type silicon target.

**Keywords:** Silicon nitride; Reactive sputtering; Thin films; Nanostructures

**Received:** 20 August 2024; **Revised:** 22 October 2024; **Accepted:** 29 October; **Published:** 1 January 2025

## 1. Introduction

Silicon nitride (Si<sub>3</sub>N<sub>4</sub>) is widely used as a hard optical material with excellent piezoelectric response [1-3]. In addition to its many photonic applications, the Si<sub>3</sub>N<sub>4</sub> and SiN<sub>1.3</sub> films are employed in the surface loading of crystalline silicon solar cells, high-frequency piezoelectric transducers, biomedical applications and nanostructures [4-8]. Silicon nitride is an important insulating material for light emitting diodes and transistors as well as for insulating gate applications [9]. Si<sub>3</sub>N<sub>4</sub> exhibits high resistivity (~10<sup>13</sup> Ω.cm), dielectric constant of 7.0 and wide energy gap (5.06-5.25 eV) [10,11]. It can be found in two main structural phases, α-Si<sub>3</sub>N<sub>4</sub> and β-Si<sub>3</sub>N<sub>4</sub> those are both hexagonal [12,13]. The chemical bonding of both phases is attributed to the interference of sp<sup>3</sup> hybrid orbitals of silicon atoms with the sp<sup>2</sup> hybrid orbitals of nitrogen atoms [14]. The fundamental unit of Si<sub>3</sub>N<sub>4</sub> lattice is the SiN<sub>4</sub> tetragon as the Si atom is located at the center of the tetragon while four N atoms are located at the corners [15]. The SiN<sub>4</sub> tetragons are connected throughout the corners as each N atom is shared by three tetragons. Hence, each N atom will have three neighboring Si atoms [16,17].

Similar to most semiconductors, the intrinsic conductivity can be changed into extrinsic semiconductors by doping with n-type or p-type dopants to serve certain photonics and optoelectronics applications [18,19]. Obviously, the main difference between the two types of the conductivity in semiconductors may determine the structural, optical and electrical properties of the silicon compounds, such as Si<sub>3</sub>N<sub>4</sub> and SiO<sub>2</sub>, made from n-type or p-type silicon atoms. Therefore, the fact that the holes are the majority charge carriers in a p-type semiconductor should be carefully considered when atoms are ejected from such material to bond to other atoms and form new compound [20]. Regardless that both hole and electron have the same electrical charge, they are different in their masses and hence different in their effects on the structural characteristics of the silicon-based compound [1,4,8].

In this work, the effect of conductivity type of silicon target on the spectroscopic characteristics of the silicon nitride nanostructures prepared by dc reactive magnetron sputtering technique was introduced.

## 2. Experimental Part

In this study, silicon nitride thin films were deposited on glass and metallic (titanium) substrates using a homemade dc reactive sputtering system. Both types of silicon wafers (n-type and p-type) were used as targets. These targets and substrates were cleaned with ethanol and distilled water before the deposition process. The electric discharge of the argon was used to generate plasma required for sputtering. The operation parameters were classified into two groups: constant and variable. The

constant parameters include the vacuum pressure, discharge voltage, discharge current, deposition temperature, and inter-electrode distance. The variable parameters include the deposition time and Ar:N<sub>2</sub> gas mixing ratio for both types of silicon wafer conductivity. The inter-electrode distance was optimized at 4 cm. Figure (1) shows the optical microscopic images of two films deposited on Ti substrate using gas mixing ratio of 70:30 from n-type and p-type silicon targets.

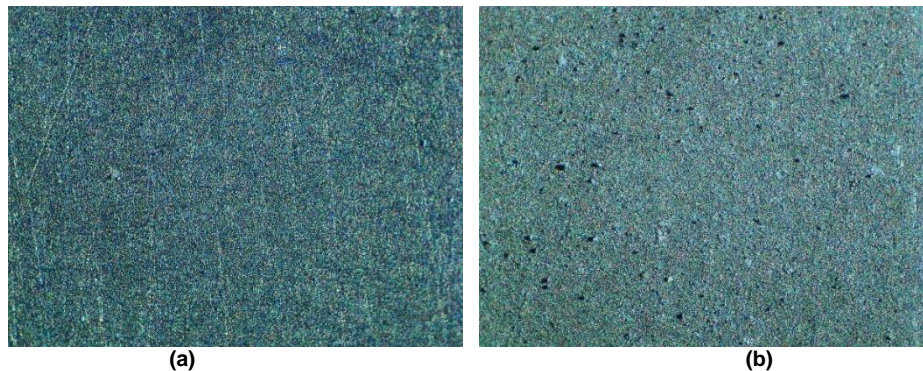


**Fig. (1) Optical microscope images of Si<sub>3</sub>N<sub>4</sub> thin films prepared from (a) n-type Si target and (b) p-type Si target and deposited on Ti substrates using gas mixing ratio of 70:30**

As the n-type silicon wafer was used mounted on the cathode as a target, the deposition chamber was initially evacuated down to 0.001 mbar and then the gas mixture of Ar:N<sub>2</sub> with mixing ratio of 50:50 was pumped into the chamber to prepare samples after different deposition times. The gas mixture pressure was about 0.15 mbar, the discharge voltage was 730 V and the discharge current was 50 mA. The mixing ratio was changed to 70:30. This procedure was repeated when the p-type silicon wafer was used. Both electrodes were cooled by circulating water through the inner channels of them. The nanopowders were extracted from the prepared thin film samples by the conjunctional freezing-assisted ultrasonic method.

The spectroscopic characteristics of the prepared samples were introduced by the UV-visible and Fourier-transform infrared (FTIR) spectroscopy.

The thickness of the prepared films was determined by the laser fringes method as 1 mW semiconductor lasers (532 and 632 nm) was used to generate concentric fringes and then determine the film thickness using the following relation [21]:

$$t = \frac{\Delta x}{x} \cdot \frac{\lambda}{2} \quad (1)$$

where  $\Delta x$  is the spacing between two adjacent bright fringes,  $x$  is the width of a bright fringe,  $\lambda$  is the wavelength of laser used

### 3. Results and Discussion

Figure (2) shows the FTIR spectra of the silicon nitride thin films prepared using two silicon targets with different types of conductivity (n- and p-type) and gas mixing ratio of 70:30. Two apparent peaks can be seen in Fig. (2a) at 958.56 and 1103.21 cm<sup>-1</sup>, while similar peaks in Fig. (2b) can be seen at 958.56 and 1097.42 cm<sup>-1</sup>. These peaks are ascribed to the vibration modes of the Si-N bonds in silicon nitride molecule. All peaks seen within 1400-3600 cm<sup>-1</sup> are attributed to the environmental contaminations those reached the samples before the FTIR tests [22].

Figure (3) shows the absorption spectra of the thin film samples prepared after different deposition times (1, 1:30, 2, 2:30 and 3 hrs) in the spectral range of 300-800 nm. It is obvious that the shorter deposition times produces samples with lower thickness and hence lower absorbance. This is typical behavior as the shorter deposition time leads to growth of fewer number of layers forming the thin film. As shown in Fig. (3a), the sample prepared after deposition time of 1 hr shows an absorption peak at 400 nm and this peak is slightly shifted towards longer wavelengths as the deposition time is increased. Beyond 400 nm, all samples show low absorption in the visible region (450-700nm). On the other hand, figure (3b) shows that all samples exhibit high absorption in the UV region and the absorbance decreases to reach a minimum at about 490 nm. Then, the absorbance starts to increase and an absorption peak can be seen around 685 nm.

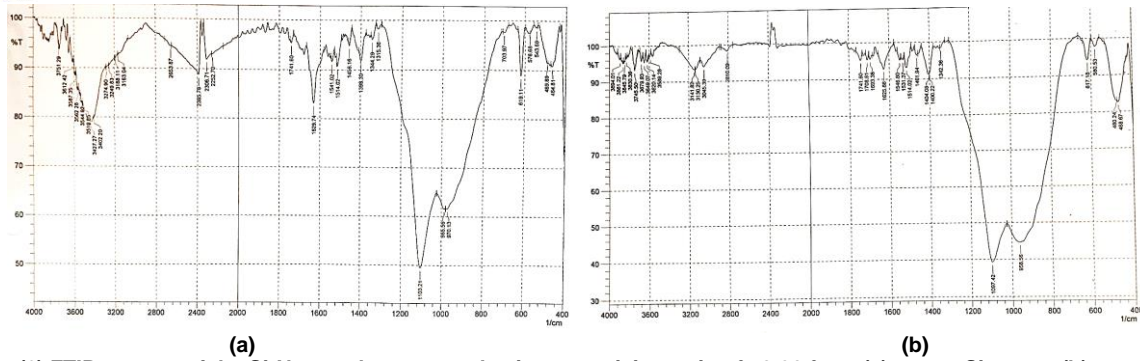


Fig. (2) FTIR spectra of the  $\text{Si}_3\text{N}_4$  samples prepared using gas mixing ratio of 70:30 from (a) n-type Si target, (b) p-type Si target

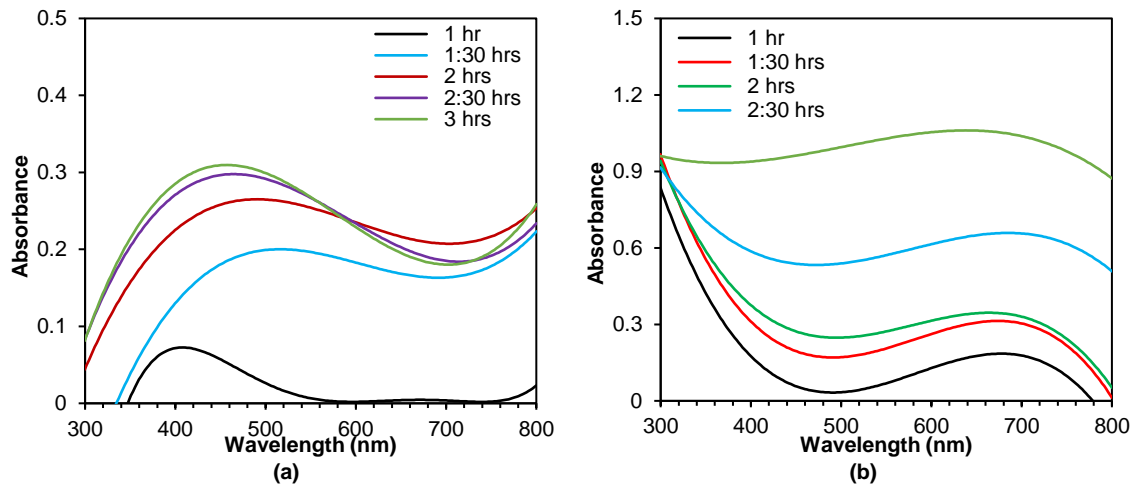


Fig. (3) Absorption spectra of the  $\text{Si}_3\text{N}_4$  samples prepared using gas mixing ratio of 70:30 from (a) n-type Si target, (b) p-type Si target

The energy band gap of silicon nitride is ranging in 4.55-5.30 eV. Figure (4) shows the variation of energy band gap of the prepared  $\text{Si}_3\text{N}_4$  samples with deposition time. It is clear that the variation in the energy band gap of the samples prepared from p-type Si target is smaller than that of samples prepared from n-type Si target. In general, increasing film thickness leads to create energy states within the band gap of the silicon nitride and hence decrease the energy band gap [23]. For the samples prepared from n-type silicon target, as the electrons are the majority charge carriers, then the majority silicon atoms sputtered from the target are bonded to nitrogen atoms to form  $\text{Si}_3\text{N}_4$  molecules. This bonding is supported by the availability of electrons ready for covalent bonding. Consequently, the number of silicon nitride molecules is relatively large and the probability of the formation of intra-band states is decreasing with film thickness and hence the energy band gap is increased to reach its maximum at 4.2 eV before decreases with increasing film thickness due to the formation of intra-band states at large thickness.

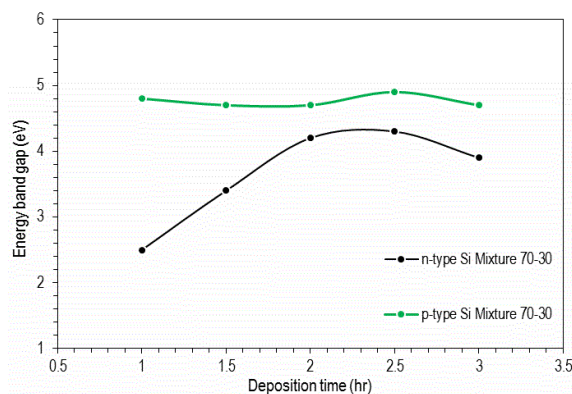


Fig. (4) Relation between energy band gap and deposition time for the  $\text{Si}_3\text{N}_4$  samples prepared using 70:30 mixing ratio from n-type and p-type Si targets

On the other hand, the silicon atoms sputtered from p-type silicon target have the holes as the majority charge carriers, therefore, the concentration of electrons available for bonding is relatively low and hence the number of silicon nitride molecules is relatively small. Accordingly, the probability of the formation of intra-band states is low too but the energy band gap is ranging in the range 4.75-4.9eV.

#### 4. Conclusion

In concluding remarks, the type of conductivity of silicon target used in the dc reactive sputtering technique has a reasonable role in determining the spectroscopic characteristics of the silicon nitride thin films prepared by this technique. Using p-type silicon target would produce  $\text{Si}_3\text{N}_4$  films with lower tendency to adsorb water vapor and other constituents of the atmospheric air, higher absorbance in the visible range 400-700nm, and lower variation in the energy band gap with film thickness than the  $\text{Si}_3\text{N}_4$  films prepared from n-type silicon target. These results are highly required to assess the prepared  $\text{Si}_3\text{N}_4$  thin films for photonics, biomedical and gas sensing applications employing these films.

#### References

- [1] P.M. Martin, "Introduction to Surface Engineering and Functionally Engineered Materials", John Wiley & Sons, Inc. (NJ, 2011) 262-264.
- [2] F.J. Kadhim and A.A. Anber, "Microhardness of Nanostructured  $\text{Si}_x\text{N}_{1-x}$  Thin Films Prepared by Reactive Magnetron Sputtering", *Iraqi J. Appl. Phys.*, 12(2) (2016) 15-19.
- [3] S.M. Sze, "Current transport and maximum dielectric strength of silicon nitride films", *J. Appl. Phys.*, 38 (1967) 2951-2955.
- [4] O.A. Hammadi, M.K. Khalaf and F.J. Kadhim, "Fabrication and Characterization of UV Photodetectors Based on Silicon Nitride Nanostructures Prepared by Magnetron Sputtering", *Proc. IMechE, Part N, J. Nanomater. Nanoeng. Nanosys.*, 230(1) (2016) 32-36.
- [5] H. Lorentz et al., "Characterization of low temperature  $\text{SiO}_2$  and  $\text{Si}_3\text{N}_4$  films deposited by plasma enhanced evaporation", *J. Vac. Sci. Technol. B*, 9 (1991) 208-214.
- [6] F.J. Kadhim and A.A. Anber, "Fabrication of nanostructured silicon nitride thin film gas sensors by reactive direct current magnetron sputtering", *Proc. IMechE, Part N, J. Nanomater. Nanoeng. Nanosys.*, 231(4) (2017) 173-178.
- [7] J.G. Simmons, "Conduction in thin dielectric films", *J. Phys. D: Appl. Phys.*, 4 (1971) 613-657.
- [8] S.W. Hseih et al., "Properties of plasma-enhanced chemical-vapor-deposited a- $\text{SiN}_x\text{:H}$  by various dilution gases", *J. Appl. Phys.*, 76 (1994) 3645-3655.
- [9] E.C. Paloura, J. Lagowski and H.C. Gatos, "Growth and electronic properties of thin  $\text{Si}_3\text{N}_4$  films grown on Si in a nitrogen glow discharge", *J. Appl. Phys.*, 69 (1991) 3995-4002.
- [10] F.J. Kadhim and A.A. Anber, "Fabrication of Nanostructured Silicon Nitride Films by Reactive DC Magnetron Sputtering for Gas Sensing Applications", *Proc. IMechE, Part N, J. Nanoeng. Nanosys.*, 231(4) (2017) 173-178.
- [11] B.K. Nasser and M.A. Hameed, "Narrow Emission Linewidth of Highly-Pure Silicon Nitride Nanoparticles in Different Dye Solutions as Random Gain Media", *Nonl. Opt. Quant. Opt.*, 35(1-2) (2020) 99-105.
- [12] O.A. Hammadi, "New Technique to Synthesize Silicon Nitride Nanopowder by Discharge-Assisted Reaction of Silane and Ammonia", *Mater. Res. Exp.*, 8(8) (2021) 085013.
- [13] X.F. Zhang, P.G. Wen and Y. Yan, "Silicon nitride thin films deposited by DC pulse reactive magnetron sputtering", *Proc. SPIE 7995, 7<sup>th</sup> Int. Conf. on Thin Film Phys. Appl.*, 17 February 2011, paper no. 79951M.
- [14] S.V. Deshpande et al., "Optical properties of silicon nitride films deposited by hot filament chemical vapor deposition", *J. Appl. Phys.*, 77(12) (1995) 6534-6541.
- [15] O.A. Hammadi, M.K. Khalaf and F.J. Kadhim, "Silicon Nitride Nanostructures Prepared by Reactive Sputtering Using Closed-Field Unbalanced Dual Magnetrons", *Proc. IMechE, Part L, J. Mater.: Design and Applications*, 231(5) (2017) 479-487.
- [16] A.A. Anber and F.J. Kadhim, "Preparation of Nanostructured  $\text{Si}_x\text{N}_{1-x}$  Thin Films by DC Reactive Magnetron Sputtering for Tribology Applications", *Silicon*, 10(3) (2018) 821-824.
- [17] B.K. Nasser and M.A. Hameed, "Structural Characteristics of Silicon Nitride Nanostructures Synthesized by DC Reactive Magnetron Sputtering", *Iraqi J. Appl. Phys.*, 15(4) (2019) 33-36.
- [18] F.J. Kadhim, O.A. Hammadi and A.A. Anber, "Spectroscopic Study of Chromium-Doped Silicon Nitride Nanostructures Prepared by DC Reactive Magnetron Sputtering", *Iraqi J. Appl. Phys.*, 17(2) (2021) 9-12.
- [19] O.A. Hammadi, M.K. Khalaf, F.J. Kadhim and B.T. Chiad, "Operation Characteristics of a Closed-Field Unbalanced Dual-Magnetrons Plasma Sputtering System", *Bulg. J. Phys.*, 41(1) (2014) 24-33.
- [20] D.A. Taher and M.A. Hameed, "Effect of Target Conductivity Type on Optical Constants of Silicon Nitride Thin Films Prepared by DC Reactive Sputtering", *Iraqi J. Appl. Phys. Lett.*, 6(3) (2023) 15-18.
- [21] M. Ohring, "The Materials Science of Thin Films", Academic Press (San Diego, 1992) Ch. 4, 182.
- [22] N.N. Greenwood and E.J.F. Ross, "Index of Vibrational Spectra of Inorganic and Organometallic Compounds", vol. III, The Butterworth Group (London, 1966) 800, 1078.
- [23] T.E. Cook Jr et al., "Band offset measurements of the  $\text{Si}_3\text{N}_4/\text{GaN}$  (0001) interface", *J. Appl. Phys.*, 94(6) (2003) 3949-3954.